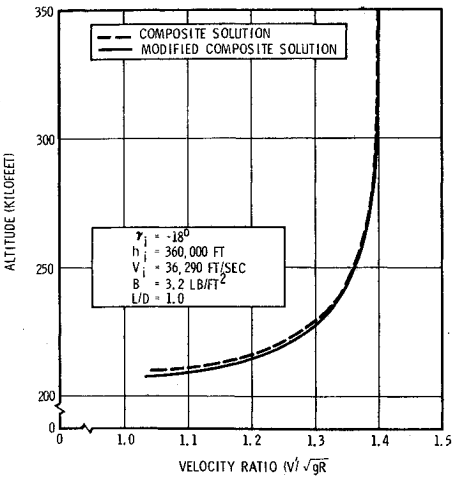

Fig. 3 Altitude vs velocity ratio—first descending arc.

and the exact solution for maximum and minimum points is given in Table 2. Agreement is surprisingly good for this case as the difference between numerical integration and the matched asymptotic solution is only about 3% at the fourth extremal point (the second peak point).

It is important to point out that our numerical solution for the altitude of the first peak results in $\beta h' = 24$ instead of the value of about 15.5 obtained by Loh (Fig. 2 of Ref. 5, Fig. 3 of Ref. 4). The difference is probably caused by the constant gravity assumption of Loh's approximations.

Further insight into the differences between the matched asymptotic approach and Loh's approximate solution may be provided by expanding Loh's solution in powers of the small parameter ϵ and comparing the results with the present approach. Carrying out inner expansion of Eqs. (5) and (7) of Ref. 4 and using the notation of Ref. 1, we obtain

$$s_0 = \cos\gamma_i - \tfrac{1}{2}C_L\rho_i + \tfrac{1}{2}\rho C_L$$
$$V_0^2 = V_i^2 \exp[(C_D/2C_L)(\gamma_0 - \gamma_i)] \quad (8)$$

$$s_1 = (1 - 1/V_0^2)(1 - \rho_i/\rho)[\cos\gamma_i + \tfrac{1}{2}\rho C_L(1 - \rho_i/\rho)] \quad (9)$$

For the purposes of comparison, s_1 is differentiated to yield

$$\frac{ds_1}{dh^*} = s_0\left\{-\left(1 - \frac{1}{V_0^2}\right)\left(1 + \frac{\rho_i}{\rho} - \frac{\cos\gamma_i}{s_0}\right) + \frac{\rho C_D}{\sin\gamma_0}\left(1 - \frac{\rho_i}{\rho}\right)\right\} \quad (10)$$

Comparing Eq. (8) with Eqs. (31) and (37) and Eq. (10) with Eq. (30) of Ref. 1, it is evident that inner expansion of Loh's approximate solution of Ref. 4 agrees in functional form with our inner solution to the lowest order. Since Loh's solution embodies the assumptions of constant gravity as well as holding constant a group of terms during integration, his approximation does not agree with our composite solution to any order in the outer region.

In summary, the present paper demonstrates that the composite solution can be applied for calculating skipping entry trajectories and numerically confirms the quality of matched asymptotic solutions. The computational procedure is much simpler than that used by Loh[4,5] and was obtained systematically by use of a well-established asymptotic expansion procedure[6,7] rather than the heuristic approach employed by Loh. In view of the success encountered in applying asymptotic methods to lift controlled atmospheric entry problems,[8] it may be conjectured that the basic approach employed here may be extended to optimum trajectories involving skipping such as the maximum range problem considered in Ref. 9.

References

[1] Shi, Y. Y. and Pottsepp, L., "Asymptotic Expansion of a Hypervelocity Atmospheric Entry Problem," *AIAA Journal*, Vol. 7, No. 2, Feb. 1969, p. 353.

[2] Willes, R. E. et al., "An Application of Matched Asymptotic Expansions to Hypervelocity Flight Mechanics," AIAA Paper 67-598, Huntsville, Ala., 1967.

[3] Willes, R. E., "An Application of the Method of Matched Asymptotic Expansions to Ordinary and Optimal Problems in Hypervelocity Flight Dynamics," Ph.D. thesis, 1966, M.I.T., Cambridge, Mass.

[4] Loh, W. H. T., "Oscillatory Motion About Center of Gravity for a Spacecraft in Planetary Atmosphere," paper presented to the 19th Congress of the International Astronautical Federation, New York, Oct. 1968.

[5] Loh, W. H. T., "Extension of the Second-Order Theory of Entry Mechanics to Nearly Exact Solutions," *AIAA Journal*, Vol. 5, No. 10, Oct. 1967, pp. 1823–1827.

[6] Van Dyke, M., *Perturbation Methods in Fluid Mechanics*, Academic Press, New York, 1964.

[7] Cole, J. D., *Perturbation Methods in Applied Mathematics*, Ginn/Blaisdell, Waltham, Mass., 1969.

[8] Shi, Y. Y., "Matched Asymptotic Solutions for Optimun Lift Controlled Atmospheric Entry," MDAC Paper WD-1182 and AIAA Paper F1–21 to be presented at the AIAA 9th Aerospace Science Meeting, New York, New York, January 25–27, 1971.

[9] Bleick, W. E. and Faulkner, F. D., "Orbital Glider Range Maximization," *AIAA Journal*, Vol. 8, No. 1, Jan. 1970, pp. 183–185.

An Optimum Design for the Instability of Cylindrical Shells under Lateral Pressure

B. I. Hyman* and A. W. Lucas Jr.†
The George Washington University, Washington, D.C.

I. Introduction

The problem of determining the strongest shell for a given weight is an out-growth of the problem treated by Tadjbakhsh and Keller[1] who determined the shape of a column which extremized the buckling load for a given weight and length. Taylor[2] subsequently showed that the governing equation of Ref. 1 for extremizing the eigenvalue can be derived from an energy functional. This method was applied by Huang and Sheu[3] to a thin-walled column under its own weight and by Wu[4] to a circular arch under lateral pressure.

The direct application of these concepts to buckling of two-dimensional structures does not appear to be very fruitful, because of the complexity of the resulting nonlinear partial differential equations. As an alternative procedure, solutions can be generated for a large number of geometries and the optimum chosen by examination. However, this procedure is very inefficient in comparison to a direct determination of the optimum by extremizing the eigenvalue, provided that the mathematical complexities associated with the latter approach can be overcome.

Optimum designs based on a direct extension of Refs. 1, 3, and 4 involve the determination of shape functions which

Received June 8, 1970; revision received December 22, 1970. This paper is based on a thesis submitted to The George Washington University in partial fulfillment of the requirements for the M.S. degree. The research was supported by NASA Grant NGR 09-010-053.

* Associate Professor, Department of Civil, Mechanical, and Environmental Engineering.

† Graduate Research Assistant, Department of Civil, Mechanical, and Environmental Engineering; currently with Pratt and Whitney Corp.

could lead to cross sections of zero area unless additional constraints on stress levels are imposed. In addition, the complicated shapes so determined may be impractical to fabricate, hence, a reasonable limitation on the class of permissible shape functions seems to be justifiable. Optimization with respect to scalar parameters describing the permissible shape functions should present a less formidable mathematical problem than optimization with respect to the shape function itself.

A further simplification in the analysis can be achieved by taking advantage of the result in Ref. 2 that the equations can be derived from the energy functional $\Delta\Pi$ (the second variation of the total potential energy). Since $\delta P = 0$ is equivalent to $\delta(\Delta\Pi) = 0$, where P is the buckling load,[5] the extremum of the eigenvalue P can be obtained by extremizing $\Delta\Pi$ directly. Thus the classical Rayleigh-Ritz method of extremizing $\Delta\Pi$ can be used to obtain an approximate solution for the optimum buckling load provided $\Delta\Pi$ is extremized with respect to the shape parameters as well as with respect to the displacement parameters. The optimum load found using this method will be an upper bound with respect to the chosen shape functions. However, there may exist other shape functions for which a higher buckling load is attainable.

Only the necessary condition for determining the optimum is satisfied with this method, and comparison of the results with those for equivalent constant thickness structures is needed to confirm optimality.

II. Mathematical Formulation

Consider the problem of a thin circular cylindrical shell with linearly varying thickness along the generator. The shell is simply supported and subject to external lateral pressure (see Fig. 1). During buckling the system passes from the prebuckling axisymmetric equilibrium state to the buckled or asymmetric state. The final displacements are given by

$$u_f = \bar{u}(x) + u(x,\theta), \quad v_f = v(x,\theta), w_f = \bar{w}(x) + w(x,\theta) \quad (1)$$

where u,v,w are the buckling displacements and $\bar{u}$, $\bar{w}$ are the prebuckling displacements. The expression for $\Delta\Pi$, the change in the total potential energy is[6]

$$\Delta\pi = \frac{Ea}{2(1-\nu^2)}\int_0^{2\pi}\int_0^L \left[u_x^2 + \left(\frac{w+v_\theta}{a}\right) + 2\nu u_x\left(\frac{w+v_\theta}{a}\right) + \frac{(1-\nu)}{2}\left(v_x + \frac{u_\theta}{a}\right)^2\right]hdxd\theta + \frac{E}{24a(1-\nu^2)}\int_0^{2\pi}\int_0^L \left[a^2 w_{xx}^2 + \frac{w_{\theta\theta}^2}{a^2} + 2\nu w_{xx}w_{\theta\theta} + 2(1-\nu)w_{x\theta}^2\right]h^3dxd\theta + \frac{Ea}{2(1-\nu^2)}\int_0^{2\pi}\int_0^L \times \left[\frac{\bar{w}}{a}\left(\frac{w_\theta^2}{a^2} + \nu w_x^2\right) + \bar{u}_x\left(\nu\frac{w_\theta^2}{a^2} + w_x^2\right)\right]hdxd\theta \quad (2)$$

where terms of higher order than the second in the buckling displacements have been discarded.

It can be shown that the assumptions used to derive Eq. (2) are consistent with the Donnell approximations and by requiring this expression for $\Delta\Pi$ to be stationary, we can arrive at the Batdorf[7] solution for the stability of short cylindrical

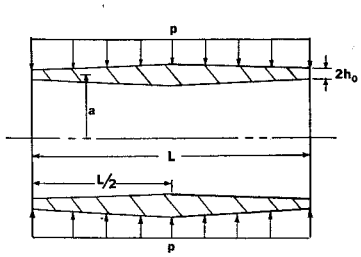

Fig. 1 Laterally loaded cylindrical shell with linearly varying wall thickness.

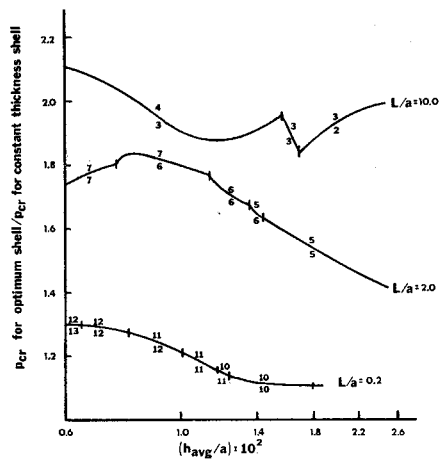

Fig. 2 Increases in buckling pressures achieved by optimum design.

shells of constant thickness. An additional assumption, which is needed only for the variable thickness shell, is that $\bar{w}/a$, $\bar{u}_x \gg \bar{w}_x$. A good first approximation for $\bar{u}_x$ and $\bar{w}$ can be obtained from membrane theory as[8]

$$\bar{u}_x = \nu ap/Eh, \quad \bar{w} = -a^2p/Eh \quad (3)$$

Then this inequality is equivalent to assuming $h/a \gg dh/dx$. The thickness variation along the length can be represented by

$$h = 2(h_0 + h_1 x/L) \qquad x \leq L/2 \quad (4)$$

where $2h_0$ is the thickness at the ends and $h_1 + 2h_0$ is the thickness at the center.

The assumed displacement functions are taken as:

$$u = \cos(n\theta)\sum_{m=1}^{K} A_m \cos(m\pi x/L)$$

$$v = \sin(n\theta)\sum_{m=1}^{K} B_m \sin(m\pi x/L) \quad (5)$$

$$w = \cos(n\theta)\sum_{m=1}^{K} C_m \sin(m\pi x/L)$$

For $K = 1$, these equations represent the exact buckling displacements for the constant thickness shell. Using the constant thickness solution as a guide, we can assume that the shell will buckle symmetrically with respect to its middle cross section. Then only the odd values of m need be included in Eq. (3) and the upper limit of integration in Eq. (2) can be changed to $x = L/2$.

Substituting Eqs. (3-5) into Eq. (2), the expression for $\Delta\Pi$ can be integrated. By requiring that the weight of the optimum shell be equal to the weight of an equivalent constant thickness shell, we obtain $h_1 = 2h_{avg} - 4h_0$ where h_{avg} is the thickness of the uniform shell. This relation is used to eliminate h_1 from the expression for $\Delta\Pi$.

The coefficients A_m, B_m, and C_m must now be chosen so as to make $\Delta\Pi$ stationary. This is done by requiring that the derivative of $\Delta\Pi$ with respect to A_m, B_m, and C_m vanish. For an optimum design we must further require that the derivative of $\Delta\Pi$ with respect to the free geometric parameter $h^* = h_0/a$ also vanish; accordingly we have

$$\partial(\Delta\Pi)/\partial A_m = \partial(\Delta\Pi)/\partial B_m = \partial(\Delta\Pi)/\partial C_m = \partial(\Delta\Pi)/\partial h^* = 0 \quad (6)$$

Thus we get a system of $3(K+1)/2 + 1$ nonlinear equations

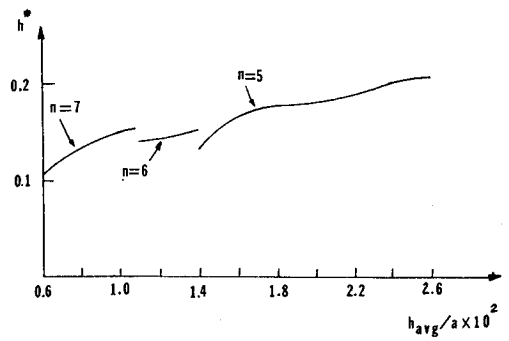

Fig. 3 Optimum thickness at the ends. $L/a = 2.0$.

to be solved for the buckling pressure, the buckling mode, and the thickness variation of the shell.

III. Results

Equations (6) were solved on an IBM 360/50 computer. For most cases, a value of $K = 15$, corresponding to eight terms in each of Eqs. (5), was sufficient to achieve convergence.

The gains achieved by optimization are shown in Fig. 2. The results show that considerable increases in the buckling pressure can be gained by varying the wall thickness. The numbers above (below) the curves in Fig. 2 refer to the number of circumferential waves in the critical mode for the optimum (constant thickness) shell. A comparison was made between the constant thickness (Batdorf) solution used here and a more exact solution.[8] For $L/a = 10.0$, it was found that the Batdorf (short shell) theory is in error by only a few percent even for a shell of this length. Figure 3 is a typical plot of the thickness at the ends versus the average thickness for $L/a = 2.0$. At the points of discontinuity of the curve, there are two geometries which yield the same buckling pressure. Each of these configurations correspond to a different number of circumferential waves in the buckled shell.

As a further result of optimization, a redistribution of buckling displacements takes place, with the maximum lateral displacement occurring between $x = 0$ and $x = L/2$.

An independent check on the validity of this method was made by disregarding the last of Eqs. (6) and using the remaining $3(K + 1)/2$ equations to generate h^* vs p_{cr} curves for a selected number of shell geometries. In all cases, the optimum found in examining these curves agreed with the optimum found directly by the procedure presented here.

References

[1] Tadjabakhsh, T. and Keller, J. B., "Strongest Columns and Isoperimetric Inequalities for Eigenvalues," *Journal of Applied Mechanics*, Vol. 29, No. 1, March 1962, pp. 159–164.

[2] Taylor, J. E., "The Strongest Column: An Energy Approach," *Journal of Applied Mechanics*, Vol. 34, No. 2, June 1967, pp. 486–487.

[3] Huang, N. C. and Sheu, C. Y., "Optimal Design of an Elastic Column of Thin-Walled Cross Section," *Journal of Applied Mechanics*, Vol. 35, No. 2, June 1968, pp. 285–288.

[4] Wu, C. H., "The Strongest Arch—A Perturbation Solution," *Journal of Applied Mechanics*, Vol. 35, No. 3, Sept. 1968, pp. 476–480.

[5] Wang, C., *Applied Elasticity*, McGraw-Hill, New York, 1953, pp. 267–271.

[6] Reynolds, T. E., "Elastic Labor Buckling of Ring-Supported Cylindrical Shells under Hydrostatic Pressure," Rept. 1614, Sept. 1962, David Taylor Model Basin.

[7] Batdorf, S. B., "A Simplified Method of Elastic Stability Analysis for Thin Cylindrical Shells," Rept. 874, 1947, NACA.

[8] Timoshenko, S. P. and Gere, J. M., "Theory of Elastic Stability," 2nd ed., McGraw-Hill, New York, 1961.

Interpretation of *n*-Dimensional Covariance Matrices

I. A. Gura* and R. H. Gersten†
The Aerospace Corporation, El Segundo, Calif.

Although error analyses constitute one of the more frequently encountered types of engineering problems, the topic is fraught with fallacies, misconceptions, and distortions. One basic difficulty occurs in attempting to interpret covariance matrices. While the usual assumption of Gaussianness is reasonable, there is a widespread tendency to assign erroneous probability confidence levels to the associated error ellipsoids. In this Note, an attempt will be made to clarify this situation.

Let x be an n-dimensional Gaussian random vector with mean $\bar{x}$ and covariance matrix C. As is well known, the probability density function for x is

$$\rho(x) = \frac{1}{(2\pi)^{n/2}(\det C)^{1/2}} \exp\left[-\frac{1}{2}(x - \bar{x})^* C^{-1}(x - \bar{x})\right] \tag{1}$$

From this it can be shown[1] that the probability that x is contained within the k-sigma hyperellipsoid

$$(x - \bar{x})^* C^{-1}(x - \bar{x}) = k^2 \tag{2}$$

is given by

$$p_n(k) = \operatorname{erf}[k/(2^{1/2})] - (2/\pi)^{1/2} \times \exp(-k^2/2)\left[k + \frac{k^3}{1\cdot 3} + \cdots + \frac{k^{n-2}}{1\cdot 3\cdot 5\cdots(n-2)}\right] \tag{3}$$

for odd n

$$p_n(k) = 1 - \exp(-k^2/2)\left[1 + \frac{k^2}{1\cdot 2} + \frac{k^4}{1\cdot 2\cdot 4} + \cdots + \frac{k^{n-2}}{1\cdot 2\cdot 4\cdots(n-2)}\right] \tag{4}$$

for even n

A graph of $p_n(k)$ vs k for selected values of n is given in Fig. 1.

When k is equal to 1 the very common "one-sigma" family of contours is encountered. It should be clear from Eqs. (3) and (4) that the probability that the random n-vector lies within the boundaries of these contours depends on n, i.e., it is $p_n(1)$ *not* $p_1(1)$ (68%) as is often incorrectly assumed. Specifically, $p_1(1)$ is the probability that any one element of the random vector lies between the intercepts of the hyperellipsoid with the corresponding coordinate axis *without* regard to where the remaining elements lie. In short, for $n > 1$, $p_n(1)$ assumes simultaneity, while $p_1(1)$ does not! Indeed, $p_n(1)$ is always smaller than $p_1(1)$ (see Fig. 1).

Another common misconception is that the square roots of the diagonal elements of the covariance matrix represent the lengths of the semiaxes of the one-sigma error hyperellipsoid. Actually, they bear no direct relationship to this contour. Note that the intercepts of the one-sigma hyperellipsoid with the coordinate axes are given by the reciprocal square roots of the diagonal elements of the *inverse* of the covariance matrix. These quantities, however, only provide an indication of the n-dimensional one-sigma error bounds and *do not*, in general, define the limits of this region. Only when the coordinate axes coincide with the principal axes does this distinction disappear.

Received August 28, 1970; revision received November 16, 1970.

* Staff Engineer, Satellite Navigation Department.

† Member Technical Staff, Satellite Navigation Department. Member AIAA.